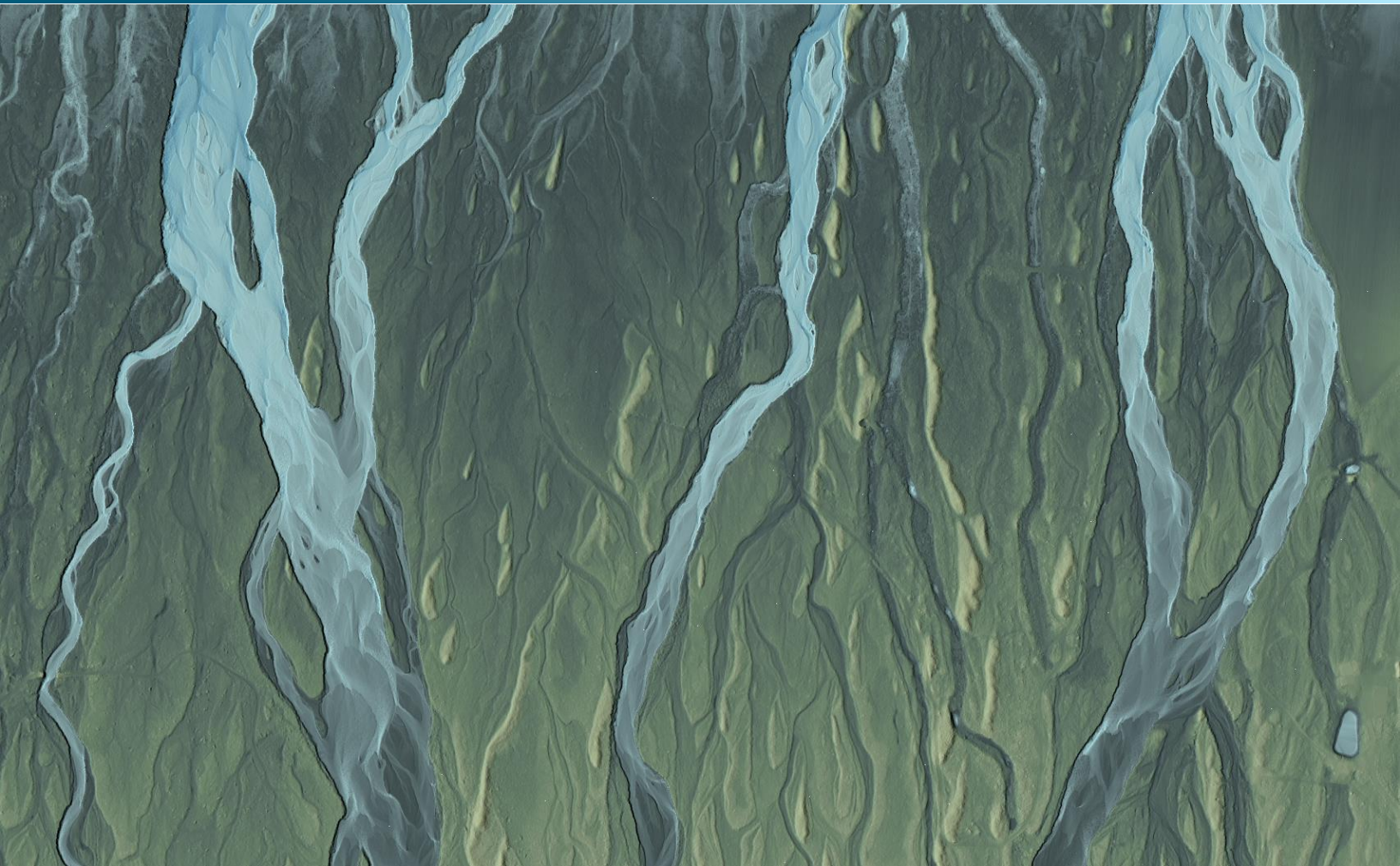


February 13, 2019



Platte River Fall 2018, Nebraska

Topobathymetric LiDAR Technical Data Report

Prepared For:



Justin Brei
Headwaters Corporation
4111 4th Avenue, Suite 6
Kearney, NE 68845
PH: 308-237-5728, ext. 4

Prepared By:



QSI Corvallis
1100 NE Circle Blvd, Ste. 126
Corvallis, OR 97330
PH: 541-752-1204

TABLE OF CONTENTS

INTRODUCTION	1
Deliverable Products	2
ACQUISITION	4
Planning.....	4
Turbidity Measurements	6
Airborne LiDAR Survey	8
Ground Control.....	10
Base Stations.....	10
Ground Survey Points (GSPs).....	10
PROCESSING	12
Topobathymetric LiDAR Data	12
Bathymetric Refraction	15
LiDAR Derived Products.....	15
Topobathymetric DEMs	15
Intensity Images.....	16
Feature Extraction	17
Hydro-flattening and Water’s Edge Breaklines	17
RESULTS & DISCUSSION	18
Bathymetric LiDAR.....	18
Mapped Bathymetry and Depth Penetration.....	18
LiDAR Point Density.....	20
First Return Point Density.....	20
Bathymetric and Ground Classified Point Densities	20
LiDAR Accuracy Assessments	23
LiDAR Non-Vegetated Vertical Accuracy	23
LiDAR Bathymetric Vertical Accuracies.....	26
LiDAR Relative Vertical Accuracy	28
CERTIFICATIONS	29
SELECTED IMAGES.....	30
GLOSSARY	33
APPENDIX A - ACCURACY CONTROLS	34

COVER PHOTO: A TOP DOWN VIEW LOOKING OVER THE BRAIDED CHANNELS OF THE PLATTE RIVER. THE IMAGE WAS CREATED FROM THE BARE EARTH MODEL AND COLORED BY ELEVATION.

INTRODUCTION

This photo taken by QSI acquisition staff shows a view of the Platte River where bathymetric check points and turbidity samples were taken.



In May 2016, Quantum Spatial (QSI) was contracted by Headwater Corporation to collect topobathymetric Light Detection and Ranging (LiDAR) data and digital imagery in the fall of 2018 as part of a multi-year contract for the Platte River in Nebraska. QSI collected bathymetric lidar and ortho-imagery for the Sub-Project Area 1 (SP1) in the fall of 2018. Traditional near-infrared (NIR) LiDAR was fully integrated with green wavelength (bathymetric) LiDAR in order to provide a seamless topobathymetric LiDAR dataset. This data collection represents part three of an ongoing four part project to aid Headwater Corporation in the Platte River Recovery Implementation Program. The program is aimed at enhancing, restoring, and protecting the habitat for the Whooping Crane, Least Tern, Piping Plover, and Pallid Sturgeon species within the project area.

This report accompanies the delivered topobathymetric LiDAR data and imagery, and documents contract specifications, data acquisition procedures, processing methods, and analysis of the final dataset including LiDAR accuracy, depth penetration, and density. Acquisition dates and acreage are shown in Table 1, a complete list of contracted deliverables provided to Headwater Corporation is shown in Table 2, and the project extent is shown in Figure 1.

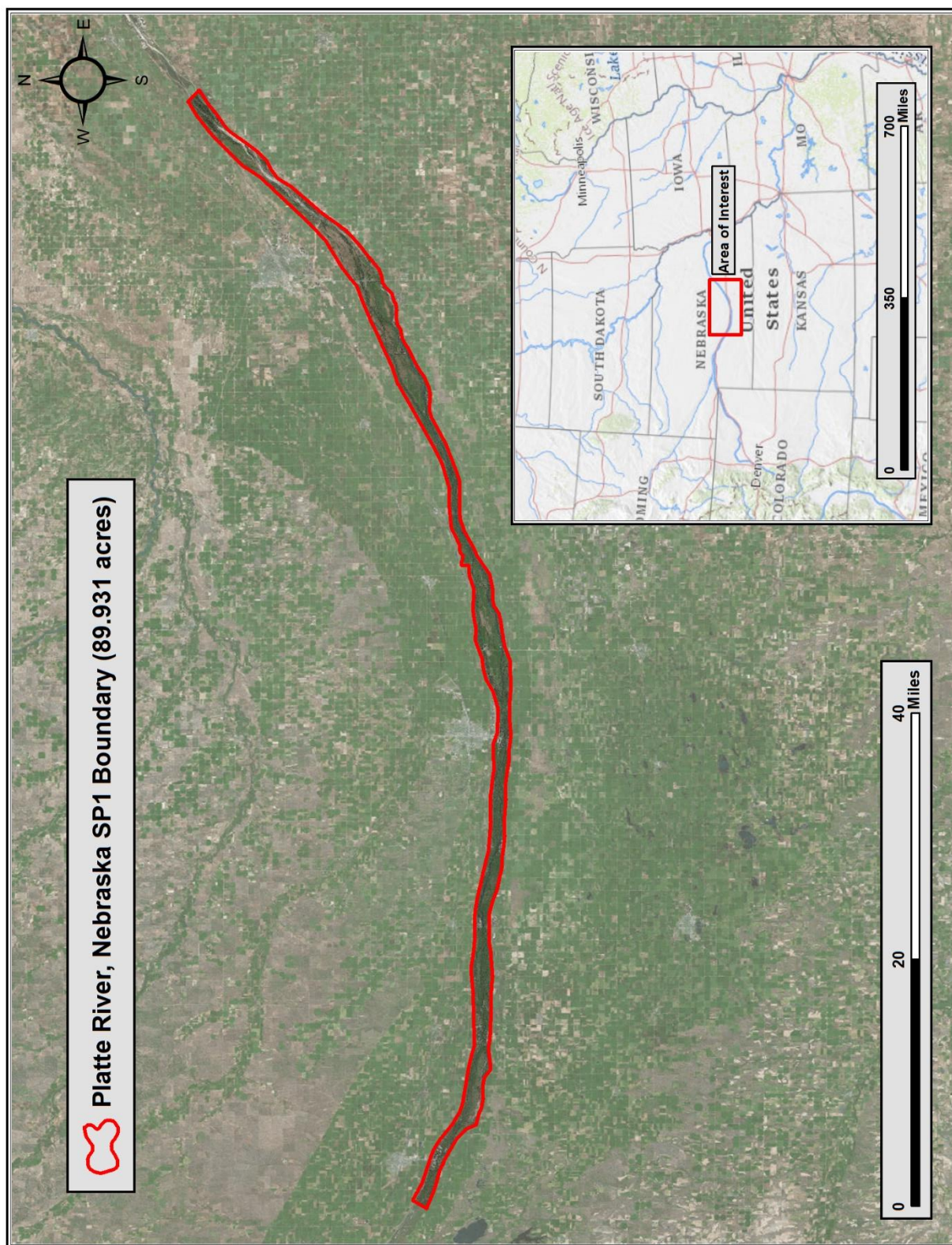
Table 1: Acquisition dates, acreage, and data types collected on the Platte River site

Project Site	Contracted Acres	Buffered Acres	Acquisition Dates	Data Type
Platte River, Nebraska	82,208	90,277	10/03/2018, 10/06/2018, 10/10/2018 – 10/13/2018	Topobathymetric LiDAR

Deliverable Products

Table 2: Products delivered to Headwater Corporation for the Platte River site

Platte River LiDAR Products	
Projection: Nebraska State Plane	
Horizontal Datum: NAD83 (2011)	
Vertical Datum: NAVD88 (GEOID03)	
Units: US Survey Feet	
Topobathymetric LiDAR	
Points	LAS v 1.4 <ul style="list-style-type: none"> All Classified Returns
Rasters	3.0 Foot ERDAS Imagine files (*.img) <ul style="list-style-type: none"> Uncropped Topobathymetric Bare Earth Digital Elevation Model (DEM) Cropped Topobathymetric Bare Earth Digital Elevation Model (DEM) Bare Earth and Water Surface Digital Elevation Model (DEM), with Hydroflattened Ponds Highest Hit Digital Surface Model (DSM) Topobathymetric Depth Model 1.5 Foot GeoTiffs <ul style="list-style-type: none"> Green Sensor Intensity Images NIR Sensor Intensity Images
Vectors	Shapefiles (*.shp) <ul style="list-style-type: none"> Project Boundary LiDAR Tile Index (1,500 ft x 1,500 ft) Raster Index Bathymetric Coverage Polygon Hydroflattened Pond Breaklines with Z values Water's Edge Breaklines without Z values (used for bathymetric refraction correction and lidar point classification) Ground Survey Shapes



QSI's Cessna Caravan



Planning

In preparation for data collection, QSI reviewed the project area and developed a specialized flight plan to ensure complete coverage of the Platte River LiDAR study area at the target combined point density of ≥ 6 points/m². Acquisition parameters including orientation relative to terrain, flight altitude, pulse rate, scan angle, and ground speed were adapted to optimize flight paths and flight times while meeting all contract specifications.

Factors such as satellite constellation availability and weather windows must be considered during the planning stage. Any weather hazards or conditions affecting the flight were continuously monitored due to their potential impact on the daily success of airborne and ground operations. In addition, logistical considerations including private property access, potential air space restrictions, channel flow rates (Figure 2 and Figure 3), and water clarity were reviewed.

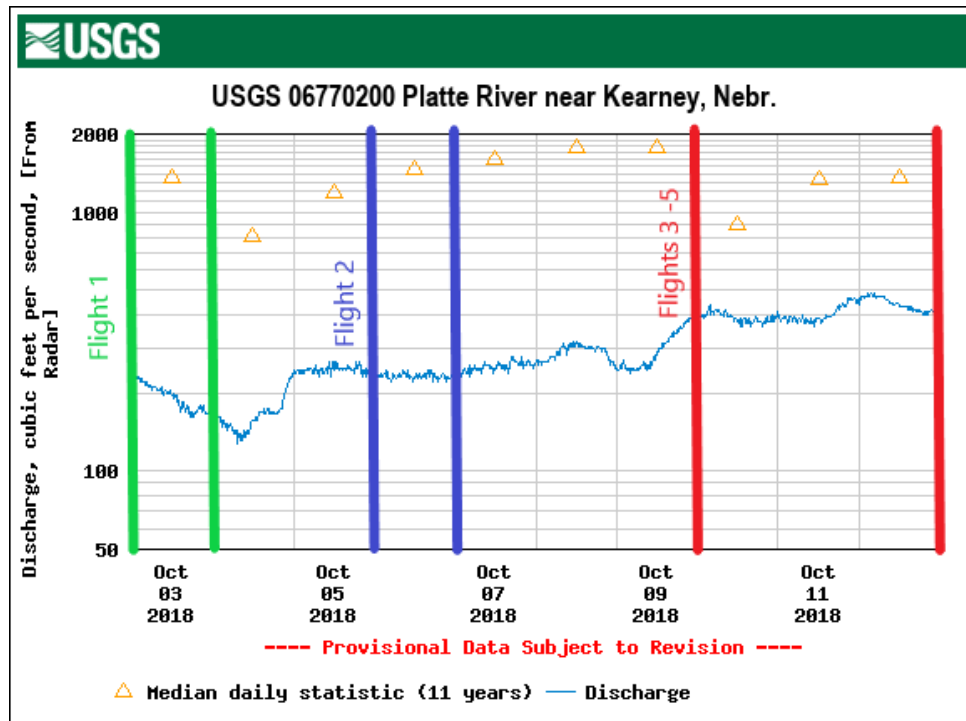


Figure 2: USGS Station 06770200 flow rates along the Platte River at the time of LiDAR acquisition.

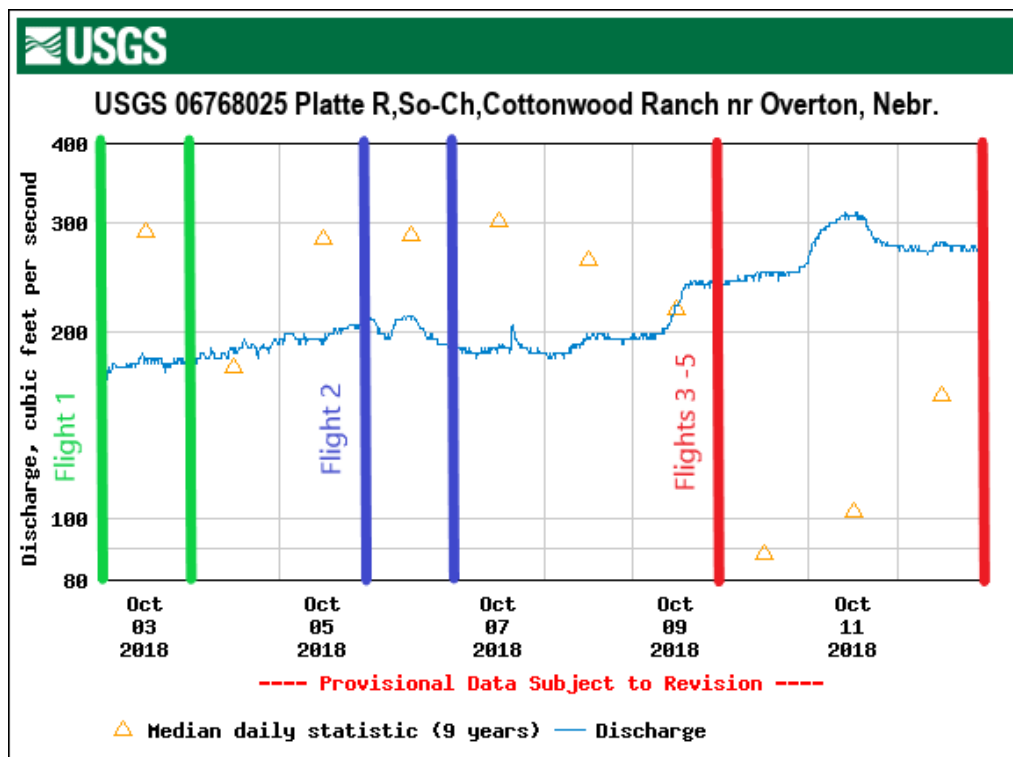


Figure 3: USGS Station 06768025 flow rates along the Platte River at the time of LiDAR acquisition.

Turbidity Measurements

In order to assess water clarity conditions prior to and during LiDAR and digital imagery collection, QSI collected turbidity measurements at three locations throughout the project site between October 3 and October 10, 2018. Turbidity observations were recorded three times at each site to confirm measurements. The table below provides turbidity results per site on each day of data collection.

Table 3: Water Clarity Observations for LiDAR flights

Turbidity Observations						
Date	Location	Longitude	Latitude	Turbidity Reading 1 (NTUs)	Turbidity Reading 2 (NTUs)	Turbidity Reading 3 (NTUs)
10/03	Plum Creek Parkway Bridge	-99° 44' 37.85"	40° 44' 08.19"	6.85	6.37	6.07
10/06	Overton Bridge RD 444	-99° 32' 23.98"	40° 40' 53.41"	3.75	4.15	4.05
10/10	B Road Near Grand Island	-98° 12' 07.66"	40° 56' 40.38"	15.2	16.0	17.2



Figure 4: Photos documenting water clarity conditions of the Platte River at the time of LiDAR acquisition, taken by QSI acquisition staff.

Airborne LiDAR Survey

The LiDAR survey was accomplished using a Riegl VQ-880-G green laser system mounted in a Cessna Caravan. The Riegl VQ-880-G uses a green wavelength ($\lambda=532$ nm) laser that is capable of collecting high resolution vegetation and topography data, as well as penetrating the water surface with minimal spectral absorption by water. The Riegl VQ-880-G contains an integrated NIR laser ($\lambda=1064$ nm) that adds additional topography data and aids in water surface modeling. The recorded waveform enables range measurements for all discernible targets for a given pulse. The typical number of returns digitized from a single pulse range from 1 to 15 for the Platte River project area. It is not uncommon for some types of surfaces (e.g., dense vegetation or water) to return fewer pulses to the LiDAR sensor than the laser originally emitted. The discrepancy between first return and overall delivered density will vary depending on terrain, land cover, and the prevalence of water bodies. All discernible laser returns were processed for the output dataset. Table 4 summarizes the settings used to yield an average pulse density of ≥ 6 pulses/m² over the Platte River project area.

Table 4: LiDAR specifications and survey settings

LiDAR Survey Settings & Specifications		
Acquisition Dates	October 03 - 13, 2018	
Aircraft Used	Cessna Caravan	
Sensor	Riegl	
Laser	VQ-880G-Green	VQ-880G-NIR
Maximum Returns	Unlimited, but typically not more than 15	Unlimited, by typically no more than 15
Resolution/Density	Average 6 pulses/m ²	Average 6 pulses/m ²
Nominal Pulse Spacing	0.4 m	0.4 m
Survey Altitude (AGL)	450 m	450 m
Survey speed	110 knots	110 knots
Field of View	40°	40°
Mirror Scan Rate	80 lines per second	Uniform point spacing
Target Pulse Rate	245 kHz	245 kHz
Pulse Length	1.5 ns	3 ns
Laser Pulse Footprint Diameter	31.5 cm	9 cm
Central Wavelength	532 nm	1064 nm
Pulse Mode	Multiple Times Around (MTA)	Multiple Times Around (MTA)
Beam Divergence	0.7 mrad	0.2 mrad
Swath Width	328 m	328 m
Swath Overlap	55%	55%
Intensity	16-bit	16-bit
Accuracy	RMSE _z ≤ 9.2 cm	RMSE _z ≤ 9.2 cm

All areas were surveyed with an opposing flight line side-lap of $\geq 50\%$ ($\geq 100\%$ overlap) in order to reduce laser shadowing and increase surface laser painting. To accurately solve for laser point position (geographic coordinates x, y and z), the positional coordinates of the airborne sensor and the attitude of the aircraft were recorded continuously throughout the LiDAR data collection mission. Position of the aircraft was measured twice per second (2 Hz) by an onboard differential GPS unit, and aircraft attitude was measured 200 times per second (200 Hz) as pitch, roll and yaw (heading) from an onboard inertial measurement unit (IMU). To allow for post-processing correction and calibration, aircraft and sensor position and attitude data are indexed by GPS time.



Top and Bottom images show QSI acquisition staff collecting submerged bathymetric check points.

Ground Control

Ground control surveys, including base station occupation and ground survey points (GSPs), were conducted to support the airborne acquisition. Base stations were occupied for the collection of ground survey points, and PP-RTX technology was used to provide redundant control for LiDAR flights.

Base Stations

Base stations were used for collection of ground survey points using real time kinematic (RTK) survey techniques. Base station locations were selected with consideration for satellite visibility, field crew safety, and optimal locations for GSP coverage. QSI utilized two base stations from the Trimble VRS Now network (Table 5, Figure 5). Steven J. Hyde (NE RLS #769) oversaw and certified the occupation of all base stations.

Table 5: Base stations utilized for the Platte River acquisition. Coordinates are on the NAD83 (2011) datum, epoch 2010.00

Base Station ID	Latitude	Longitude	Ellipsoid (meters)	Type
NEDO	40° 46' 39.11703"	-98° 22' 36.49354"	576.962	CORS
NELN	40° 46' 05.66516"	-99° 42' 43.38894"	708.806	CORS

Ground Survey Points (GSPs)

Ground survey points were collected using an RTK survey technique. For an RTK survey, a roving receiver receives corrections from a nearby base station or Real-Time Network (RTN) via radio or cellular network, enabling rapid collection of points with relative errors less than 1.5 cm horizontal and 2.0 cm vertical. RTK surveys record data while stationary for at least five seconds, calculating the position using at least three one-second epochs. All GSP measurements were made during periods with a Position Dilution of Precision (PDOP) of ≤ 3.0 with at least six satellites in view of the stationary and roving receivers. See Table 6 for QSI ground survey equipment specifications.

GSPs were collected in areas where good satellite visibility was achieved on paved roads and other hard surfaces such as gravel or packed dirt roads. GSP measurements were not taken on highly reflective surfaces such as center line stripes or lane markings on roads due to the increased noise seen in the laser returns over these surfaces. GSPs were collected within as many flightlines as possible; however, the distribution of GSPs depended on ground access constraints and monument locations and may not be equitably distributed throughout the study area (Figure 5).

Table 6: Trimble equipment identification

Receiver Model	Antenna	OPUS Antenna ID	Use
Trimble R8	Integrated Antenna R8 Model 2	TRM_R8_GNSS	Rover
Trimble Net R9	Zephyr GNSS Geodetic Model II	TRM55971.00	Base Station

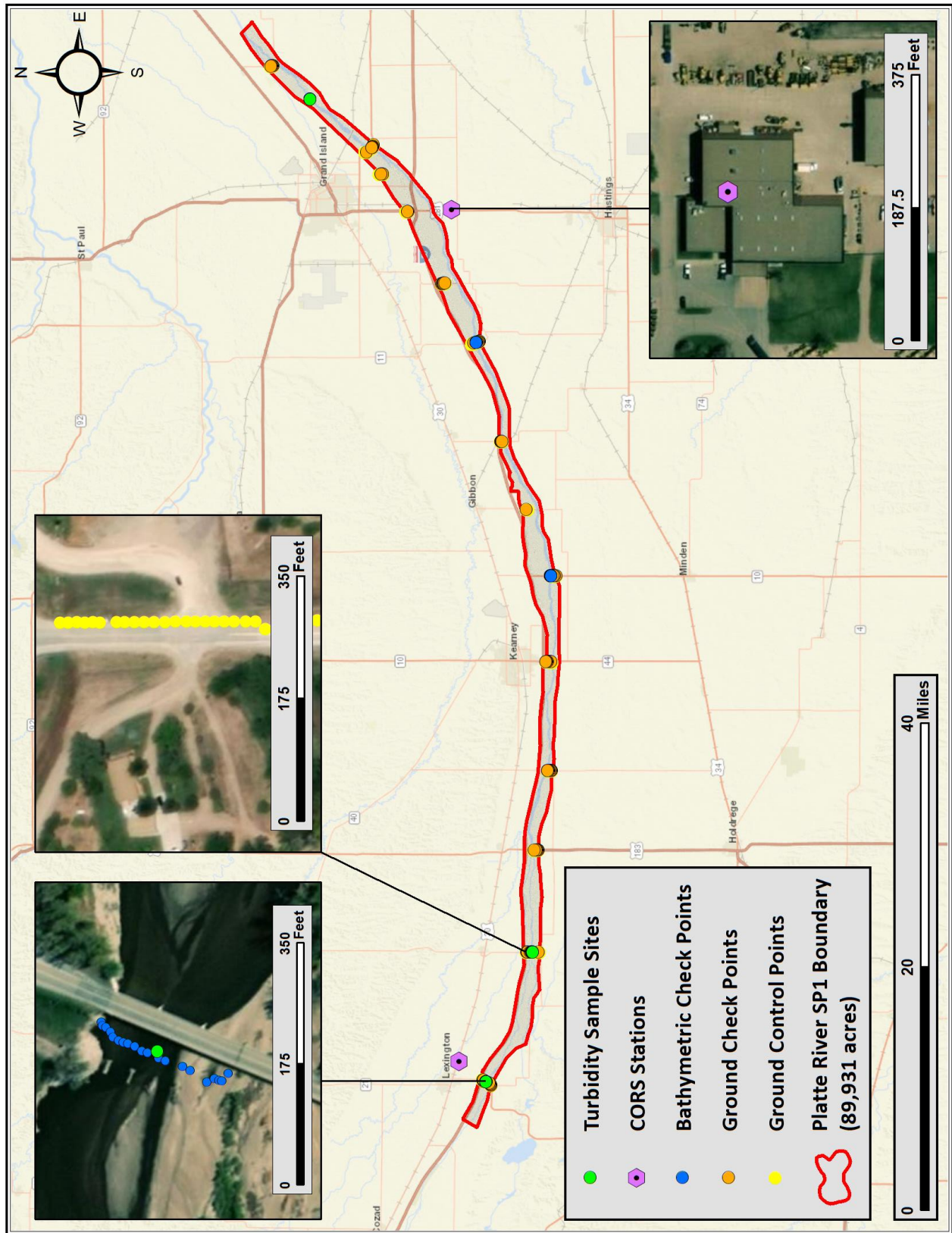
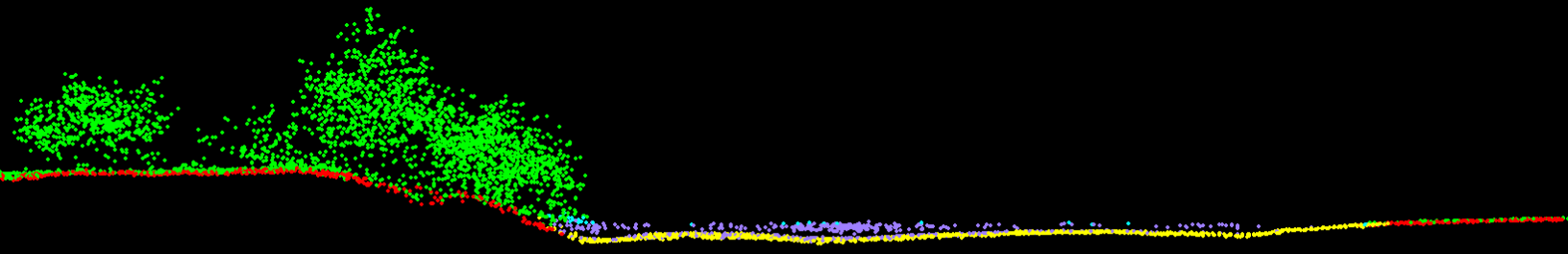


Figure 5: Ground Survey Location Map

Ground
Bathymetric Bottom
Default
Water Column
Water Surface

This 6 ft wide cross section shows a view of the Platte River point cloud colored by point classification.



Topobathymetric LiDAR Data

Upon completion of data acquisition, QSI processing staff initiated a suite of automated and manual techniques to process the data into the requested deliverables. Processing tasks included GPS control computations, smoothed best estimate trajectory (SBET) calculations, kinematic corrections, calculation of laser point position, sensor and data calibration for optimal relative and absolute accuracy, and LiDAR point classification (Table 7).

Riegl's RiProcess software was used to facilitate bathymetric return processing. Once bathymetric points were differentiated, they were spatially corrected for refraction through the water column based on the angle of incidence of the laser. QSI refracted water column points using QSI's proprietary LAS processing software, LAS Monkey. The resulting point cloud data were classified using both manual and automated techniques. Processing methodologies were tailored for the landscape. Brief descriptions of these tasks are shown in (Table 8).

Table 7: ASPRS LAS classification standards applied to the Platte River dataset

Classification Number	Classification Name	Classification Description
1	Default/Unclassified	Laser returns that are not included in the ground class, composed of vegetation and anthropogenic features
1-0	Overlap/Edge Clip	Flightline edge overlap clipped to maintain contracted scan angles
2	Ground	Laser returns that are determined to be ground using automated and manual cleaning algorithms
7	Noise	Laser returns that are often associated with birds, scattering from reflective surfaces, or artificial points below the ground surface
9	Water	NIR Laser returns that are determined to be water using automated and manual cleaning algorithms
20	Ignored Ground	Ground points proximate to water's edge breaklines; ignored for correct model creation.
40	Bathymetric Bottom	Refracted Riegl sensor returns that fall within the water's edge breakline which characterize the submerged topography.
41	Water Surface	Green laser returns that are determined to be water surface points using automated and manual cleaning algorithms.
45	Water Column	Refracted Riegl sensor returns that are determined to be water using automated and manual cleaning algorithms.

Table 8: LiDAR processing workflow

LiDAR Processing Step	Software Used
Resolve kinematic corrections for aircraft position data using kinematic aircraft GPS and static ground GPS data. Develop a smoothed best estimate of trajectory (SBET) file that blends post-processed aircraft position with sensor head position and attitude recorded throughout the survey.	POSPac MMS v.8.2
Calculate laser point position by associating SBET position to each laser point return time, scan angle, intensity, etc. Create raw laser point cloud data for the entire survey in *.las (ASPRS v. 1.4) format. Convert data to orthometric elevations by applying a geoid correction.	RiProcess v1.8.5 TerraMatch v.18
Import raw laser points into manageable blocks to perform manual relative accuracy calibration and filter erroneous points. Classify ground points for individual flight lines.	TerraScan v.18
Using ground classified points per each flight line, test the relative accuracy. Perform automated line-to-line calibrations for system attitude parameters (pitch, roll, heading), mirror flex (scale) and GPS/IMU drift. Calculate calibrations on ground classified points from paired flight lines and apply results to all points in a flight line. Use every flight line for relative accuracy calibration.	TerraMatch v.18 RiProcess v1.8.5
Apply refraction correction to all subsurface returns.	LAS Monkey 2.4.0 (QSI proprietary software)
Classify resulting data to ground and other client designated ASPRS classifications (Table 7). Assess statistical absolute accuracy via direct comparisons of ground classified points to ground control survey data.	TerraScan v.18 TerraModeler v.18
Generate bare earth models as triangulated surfaces. Generate highest hit models as a surface expression of all classified points. Export all surface models in ERDAS Imagine (.img) format at a 3.0 foot pixel resolution.	TerraScan v.18 TerraModeler v.18 ArcMap v. 10.3.1
Correct intensity values for variability and export intensity images as GeoTIFFs at a 1.5 foot pixel resolution.	ArcMap v. 10.3.1 Las Product Creator 3.0 (QSI proprietary software)

Bathymetric Refraction

Green LiDAR pulses that enter the water column must have their position corrected for refraction of the light beam as it passes through the water and its resulting decreased speed. QSI has developed proprietary software (Las Monkey) to perform this processing based on Snell's law. The first step is to develop a water surface model (WSM) from the NIR LiDAR water surface returns. The water surface model used for refraction is generated using NIR points within the breaklines defining the water's edge. Points are filtered and edited to obtain the most accurate representation of the water surface and are used to create a water surface model TIN. A TIN model is preferable to a raster based water surface model to obtain the most accurate angle of incidence during refraction.

Once the WSM is generated, the Las Monkey refraction software then intersects the partially submerged green pulses with the WSM to determine the angle of incidence with the water surface and the submerged component of the pulse vector. This provides the information necessary to correct the position of underwater points by adjusting the submerged vector length and orientation. After refraction, the points are compared against bathymetric check points to assess accuracy.

LiDAR Derived Products

Because hydrographic laser scanners penetrate the water surface to map submerged topography, this affects how the data should be processed and presented in derived products from the LiDAR point cloud. The following discusses certain derived products that vary from the traditional (NIR) specification and delivery format.

Topobathymetric DEMs

Bathymetric bottom returns can be limited by depth, water clarity, and bottom surface reflectivity. Water clarity and turbidity affects the depth penetration capability of the green wavelength laser with returning laser energy diminishing by scattering throughout the water column. Additionally, the bottom surface must be reflective enough to return remaining laser energy back to the sensor at a detectable level. It is not unexpected to have no bathymetric bottom returns in turbid or non-reflective areas. As a result, creating digital elevation models (DEMs) presents a challenge with respect to interpolation of areas with no returns. Traditional DEMs are "unclipped", meaning areas lacking ground returns are interpolated from neighboring ground returns (or breaklines in the case of hydro-flattening), with the assumption that the interpolation is close to reality. In bathymetric modeling, these assumptions are prone to error because a lack of bathymetric returns can indicate a change in elevation that the laser can no longer map due to increased depths. The resulting void areas may suggest greater depths, rather than similar elevations from neighboring bathymetric bottom returns. Therefore, QSI created a water polygon with bathymetric coverage to delineate areas with successfully mapped bathymetry. This shapefile was used to control the extent of the delivered clipped topobathymetric model to avoid false triangulation (interpolation from TIN'ing) across areas in the water with no bathymetric returns.

Intensity Images

The difference in emitted wavelengths of the NIR (1064 nm) and Green (532 nm) lasers results in variation of the intensity information returned to the sensor for each laser. Additionally, the near-infrared wavelength is subject to spectral absorption by water, which can result in no returns over water surfaces. Due to these factors, QSI created one set of intensity images from NIR laser first returns, as well as one set of intensity images from green laser first returns (Figure 6).

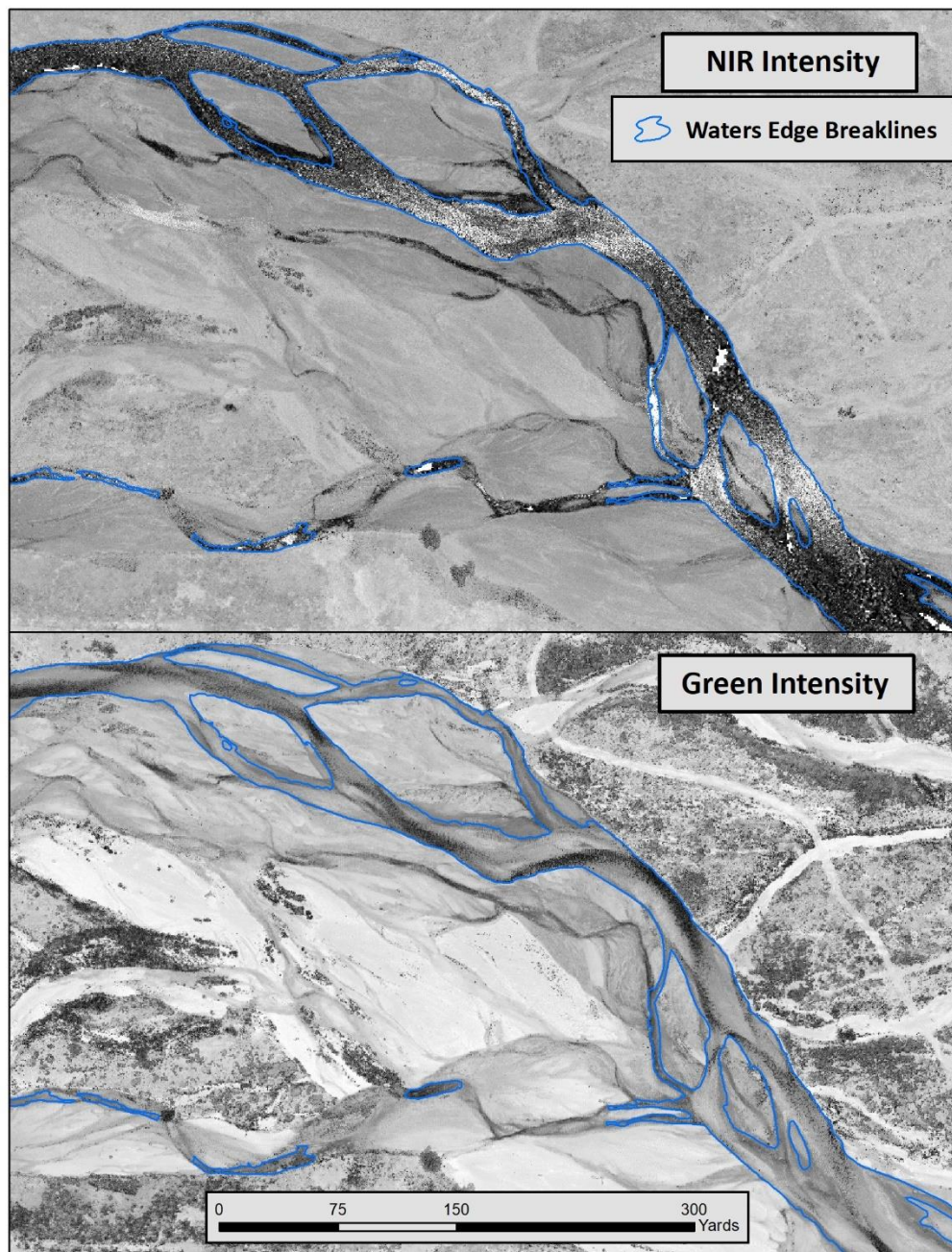


Figure 6: A comparison of Intensity Images from Green and NIR returns in the Platte River area

Feature Extraction

Hydro-flattening and Water's Edge Breaklines

Hydro-flattening of closed water bodies was performed through a combination of automated and manual detection and adjustment techniques designed to identify water boundaries and water levels. Boundary polygons were developed using an algorithm which weights LiDAR-derived slopes, intensities, and return densities to detect the water's edge. The water edges were then manually reviewed and edited as necessary.

For the Platte River SP1 project area all lakes and ponds outside of the area's main river channel were flattened to a consistent water level. The hydro-flattening process eliminates artifacts in the digital terrain model caused by both increased variability in ranges or dropouts in laser returns due to the low reflectivity of water.

Once polygons were developed, the initial ground classified points falling within water polygons were reclassified as water points to omit them from the final ground model. Elevations were then obtained from the filtered LiDAR returns to create the final breaklines.

Water boundary breaklines were then incorporated into the hydro-flattened DEM by enforcing triangle edges (adjacent to the breakline) to the elevation values of the breakline. This implementation corrected interpolation along the hard edge. Water surfaces were obtained from a TIN of the 3-D water edge breaklines resulting in the final hydro-flattened model (Figure 7).

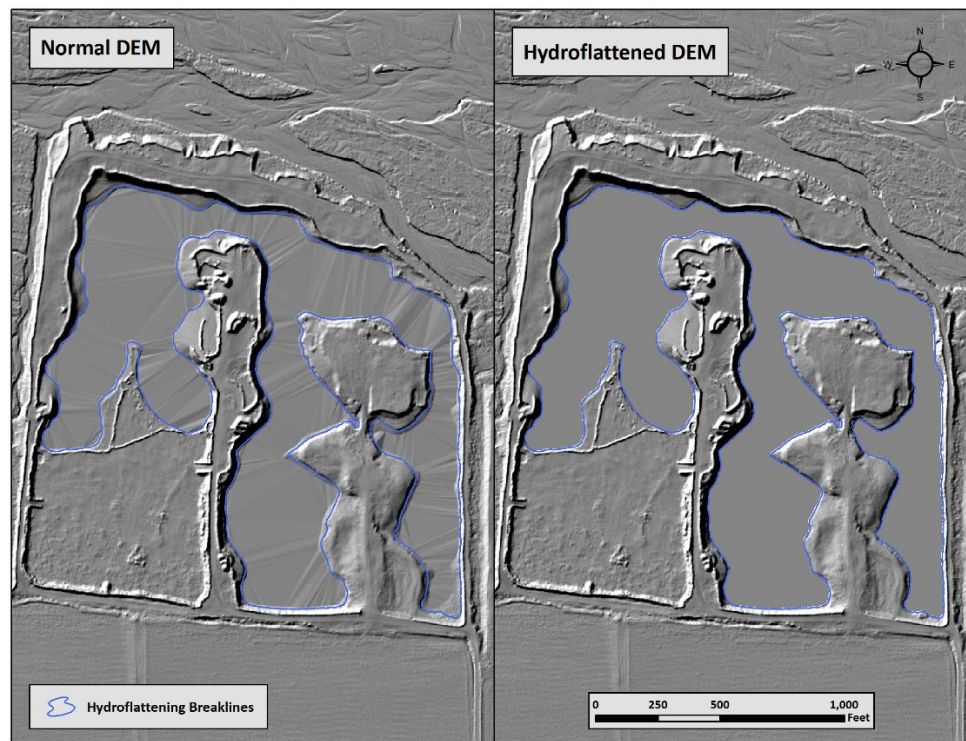
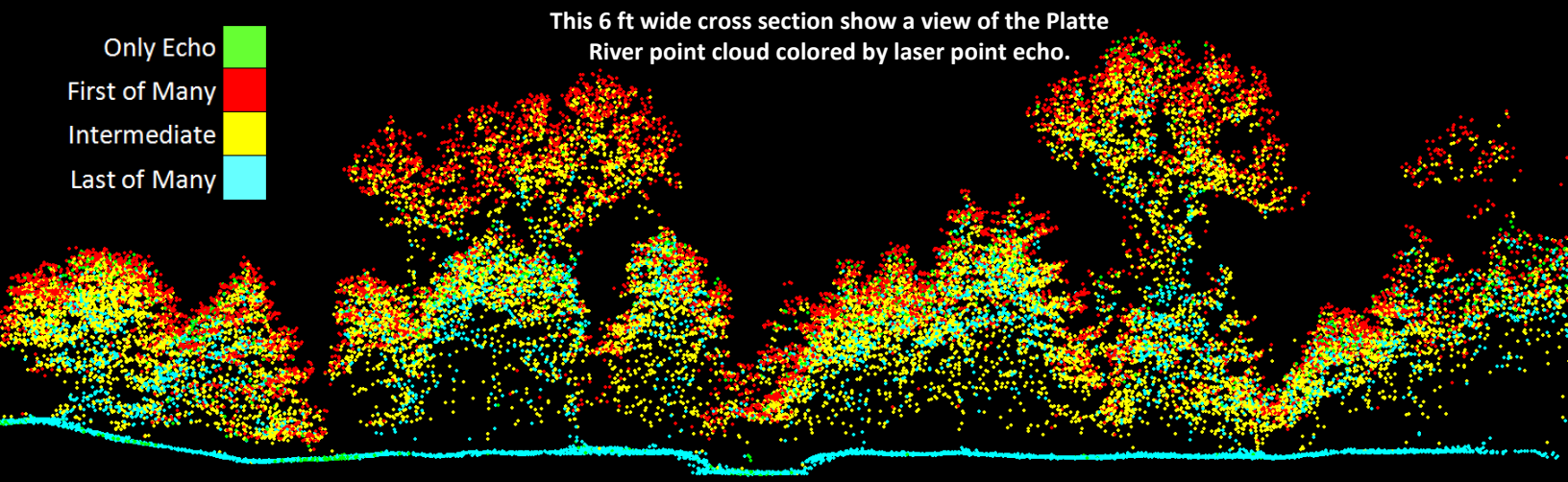


Figure 7: Example of hydroflattening in the Platte River LiDAR dataset



Bathymetric LiDAR

An underlying principle for collecting hydrographic LiDAR data is to survey near-shore areas that can be difficult to collect with other methods, such as multi-beam sonar, particularly over large areas. In order to determine the capability and effectiveness of the bathymetric LiDAR, several parameters were considered; depth penetrations below the water surface, bathymetric return density, and spatial accuracy.

Mapped Bathymetry and Depth Penetration

The specified depth penetration range of the Riegl VQ-880-G sensor is 1.5 the secchi depths; therefore, bathymetry data below 1.5x the secchi depth at the time of acquisition is not to be expected. In order to calculate overall max depth and to review depth results of bathymetric check point data, a water surface DEM raster was created by triangulating all ground and water surface points at a 3 foot pixel resolution. The triangulated topobathymetric DEM was subtracted from the water surface model to create a depth raster from which max depth was derived (Figure 8). The maximum depth recorded for the Platte River project was approximately 19.99 feet (6.09 meters).

To assist in evaluating the performance results of the sensor, a polygon layer was created to delineate areas where bathymetry was successfully mapped. Insufficiently mapped areas were identified by triangulating bathymetric bottom points with an edge length maximum of 15.2 feet (4.56 meters). This ensured all areas of no returns $> 100 \text{ ft}^2$ ($> 9 \text{ m}^2$), were identified as data voids. Overall, 76% (5,292 acres) of the mapped water within Platte River project area was identified as “covered” with 99% of the main river channels being successfully mapped.

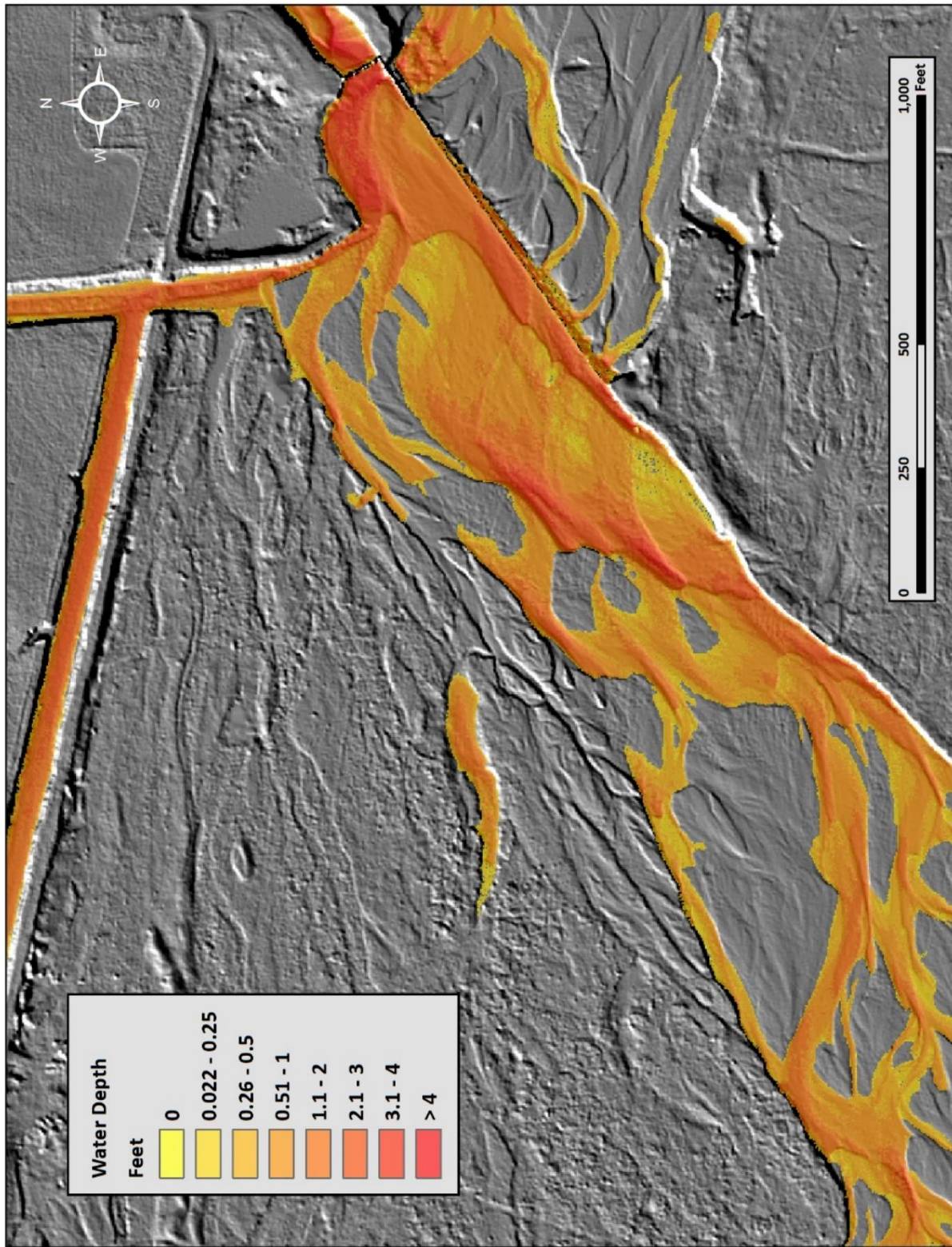


Figure 8: Platte River, Nebraska Fall 2018 Depth Map

LiDAR Point Density

First Return Point Density

The acquisition parameters were designed to acquire an average first-return density of 0.55 points/ft² (6 points/m²). First return density describes the density of pulses emitted from the laser that return at least one echo to the system. Multiple returns from a single pulse were not considered in first return density analysis. Some types of surfaces (e.g., breaks in terrain, water and steep slopes) may have returned fewer pulses than originally emitted by the laser.

First returns typically reflect off the highest feature on the landscape within the footprint of the pulse. In forested or urban areas the highest feature could be a tree, building or power line, while in areas of unobstructed ground, the first return will be the only echo and represents the bare earth surface.

The average first-return density of the Platte River LiDAR project was 1.93 points/ft² (20.73 points/m²) (Table 10, Figure 9). The statistical and spatial distributions of all first return densities per 100 m x 100 m cell are portrayed in Figure 9 and Figure 11.

Bathymetric and Ground Classified Point Densities

The density of ground classified LiDAR returns and bathymetric bottom returns were also analyzed for this project. Terrain character, land cover, and ground surface reflectivity all influenced the density of ground surface returns. In vegetated areas, fewer pulses may have penetrated the canopy, resulting in lower ground density. Similarly, the density of bathymetric bottom returns was influenced by turbidity, depth, and bottom surface reflectivity. In turbid areas, fewer pulses may have penetrated the water surface, resulting in lower bathymetric density.

The ground and bathymetric bottom classified density of LiDAR data for the Platte River project was 0.91 points/ft² (9.75 points/m²) (Figure 10). The statistical and spatial distributions ground classified and bathymetric bottom return densities per 100 m x 100 m cell are portrayed in Figure 10 and Figure 11.

Additionally, for the Platte River project, density values of only bathymetric bottom returns were calculated for areas containing at least one bathymetric bottom return. Areas lacking bathymetric returns (voids) were not considered in calculating an average density value. Within the successfully mapped area, a bathymetric bottom return density of 0.95 points/ft² (10.21 points/m²) was achieved.

Table 9: Average LiDAR point densities

Density Type	Point Density
First Returns	1.93 points/ft ² 20.73 points/m ²
Ground and Bathymetric Bottom Classified Returns	0.91 points/ft ² 9.75 points/m ²
Bathymetric Bottom Classified Returns	0.95 points/ft ² 10.21 points/m ²

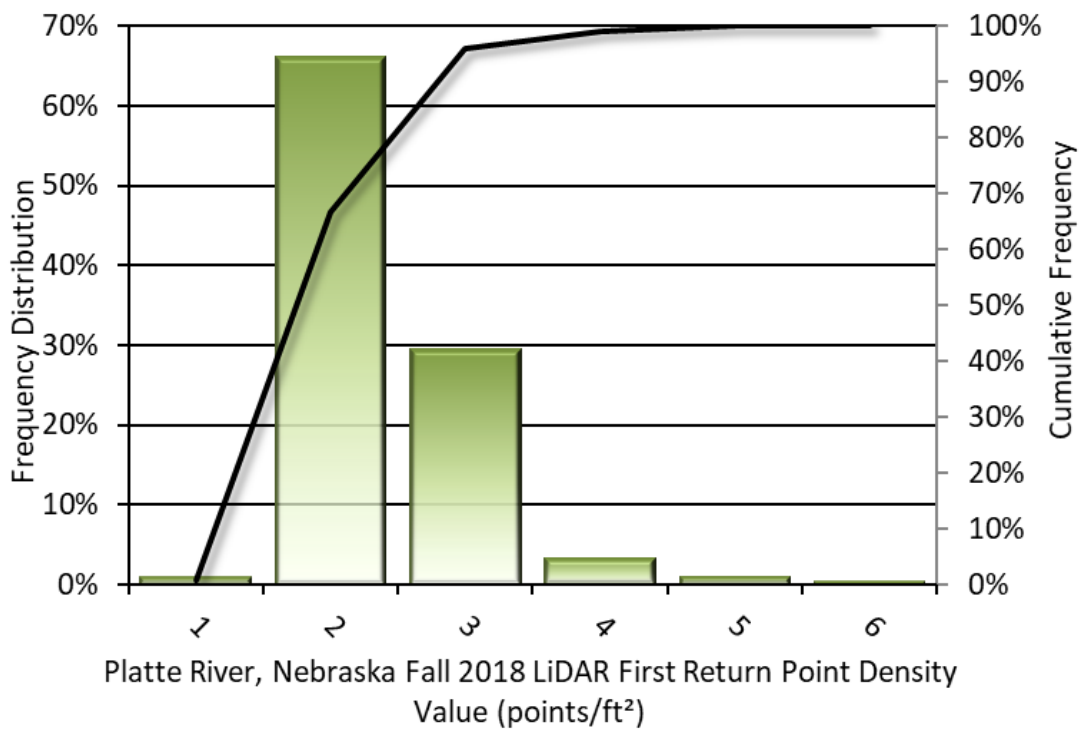


Figure 9: Frequency distribution of first return densities per 100 x 100 m cell

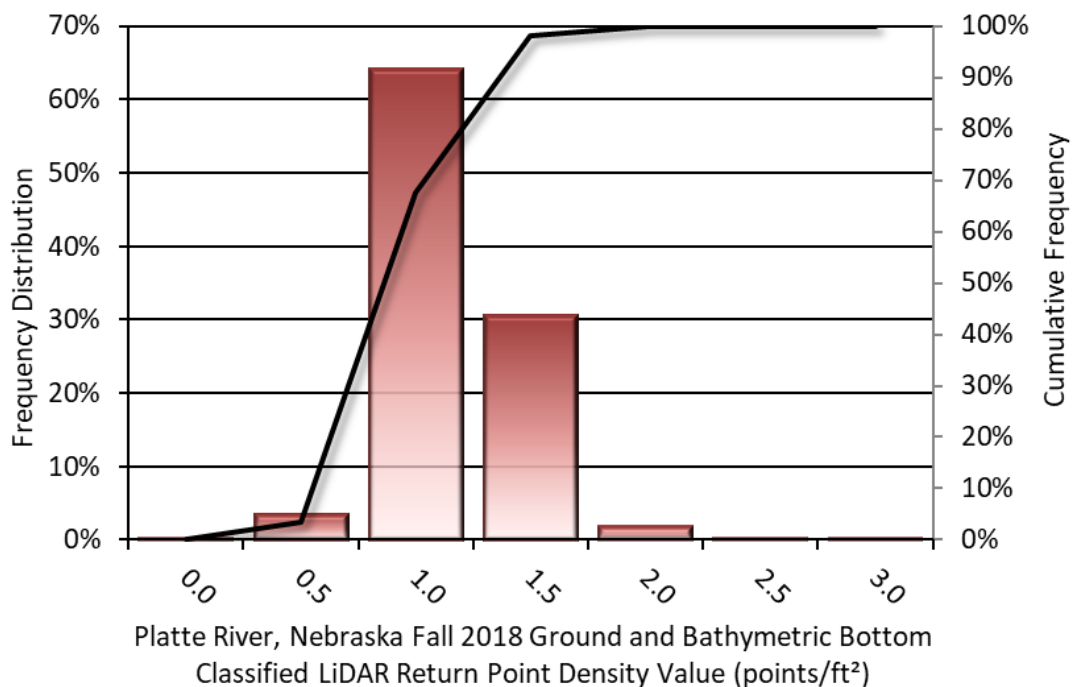


Figure 10: Frequency distribution of ground and bathymetric bottom classified return densities per 100 x 100 m cell

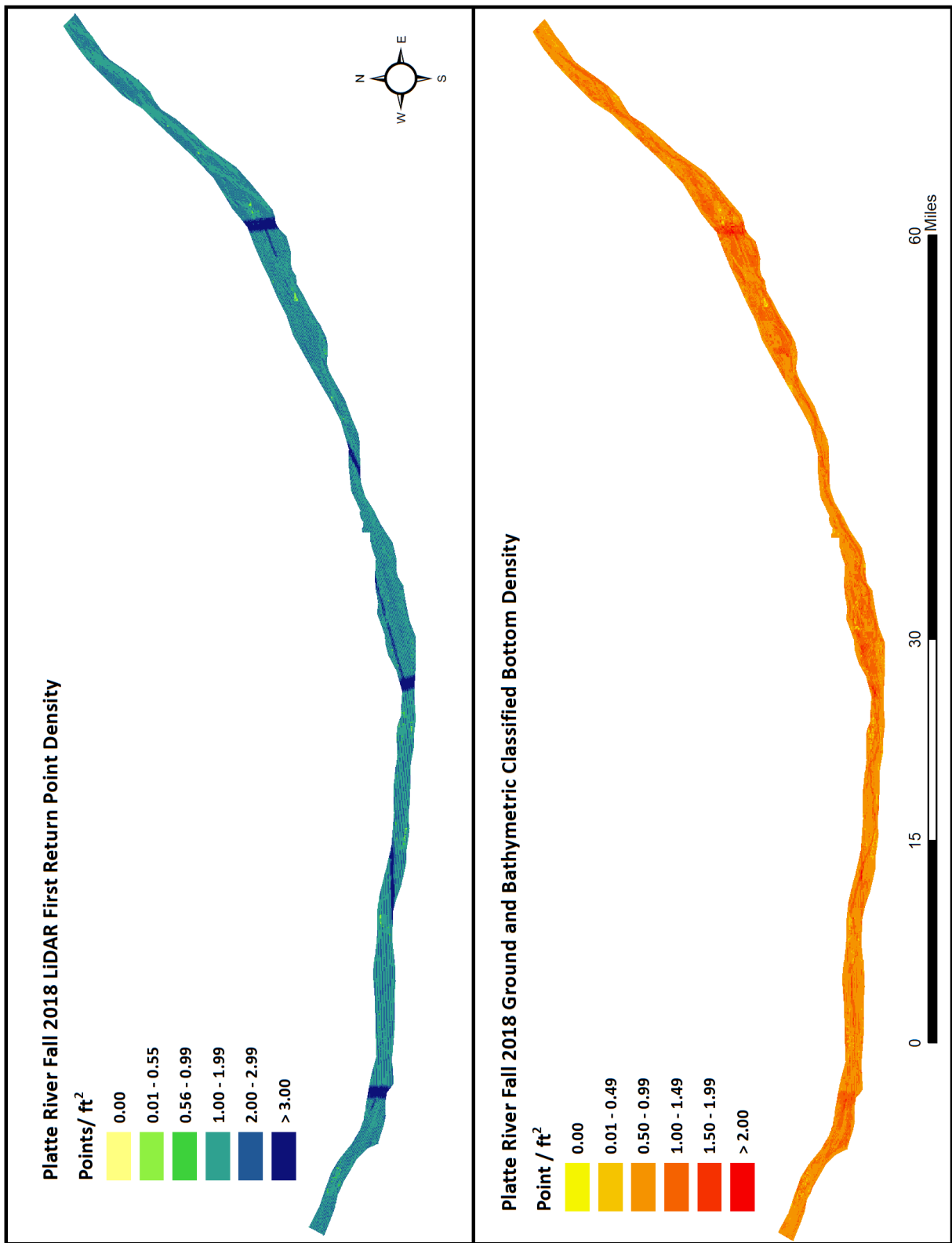


Figure 11: Density maps for the Platte River site (100 m x 100 m cells)

LiDAR Accuracy Assessments

The accuracy of the LiDAR data collection can be described in terms of absolute accuracy (the consistency of the data with external data sources) and relative accuracy (the consistency of the dataset with itself). See Appendix A for further information on sources of error and operational measures used to improve relative accuracy.

LiDAR Non-Vegetated Vertical Accuracy

Absolute accuracy was assessed using Non-vegetated Vertical Accuracy (NVA) reporting designed to meet guidelines presented in the FGDC National Standard for Spatial Data Accuracy¹. NVA compares known ground check point data that were withheld from the calibration and post-processing of the LiDAR point cloud to the triangulated surface generated by the unclassified LiDAR point cloud as well as the derived gridded bare earth DEM. NVA is a measure of the accuracy of LiDAR point data in open areas where the LiDAR system has a high probability of measuring the ground surface and is evaluated at the 95% confidence interval ($1.96 * RMSE$), as shown in Table 10.

The mean and standard deviation (sigma σ) of divergence of the ground surface model from ground check point coordinates are also considered during accuracy assessment. These statistics assume the error for x, y and z is normally distributed, and therefore the skew and kurtosis of distributions are also considered when evaluating error statistics. For the Platte River survey, 85 ground check points were withheld from the calibration and post-processing of the LiDAR point cloud, with resulting non-vegetated vertical accuracy of 0.188 feet (0.057 meters), as compared to the unclassified LAS and 0.187 feet (0.057 meters) against the bare earth DEM, with 95% confidence (Table 10, Figure 12 and Figure 13).

QSI also assessed absolute accuracy using 1,612 ground control points. Although these points were used in the calibration and post-processing of the LiDAR point cloud, they still provide a good indication of the overall accuracy of the LiDAR dataset, and therefore have been provided in Table 10 and Figure 14.

¹ Federal Geographic Data Committee, ASPRS POSITIONAL ACCURACY STANDARDS FOR DIGITAL GEOSPATIAL DATA EDITION 1, Version 1.0, NOVEMBER 2014. <http://www.asprs.org/PAD-Division/ASPRS-POSITIONAL-ACCURACY-STANDARDS-FOR-DIGITAL-GEOSPATIAL-DATA.html>.

Table 10: Absolute accuracy results

Absolute Vertical Accuracy			
	NVA - Ground Check Points (LAS)	NVA - Ground Check Points (DEM)	Ground Control Points
Sample	85 points	85 points	1,612 points
95% Confidence (1.96*RMSE)	0.188 ft	0.187 ft	0.176 ft
	0.057 m	0.057 m	0.054 m
Average	0.012 ft	0.011 ft	-0.020 ft
	0.004 m	0.003 m	-0.006 m
Median	0.013 ft	0.020 ft	-0.026 ft
	0.004 m	0.006 m	-0.008 m
RMSE	0.096 ft	0.095 ft	0.090 ft
	0.029 m	0.029 m	0.027 m
Standard Deviation (1σ)	0.096 ft	0.095 ft	0.087 ft
	0.029 m	0.029 m	0.027 m

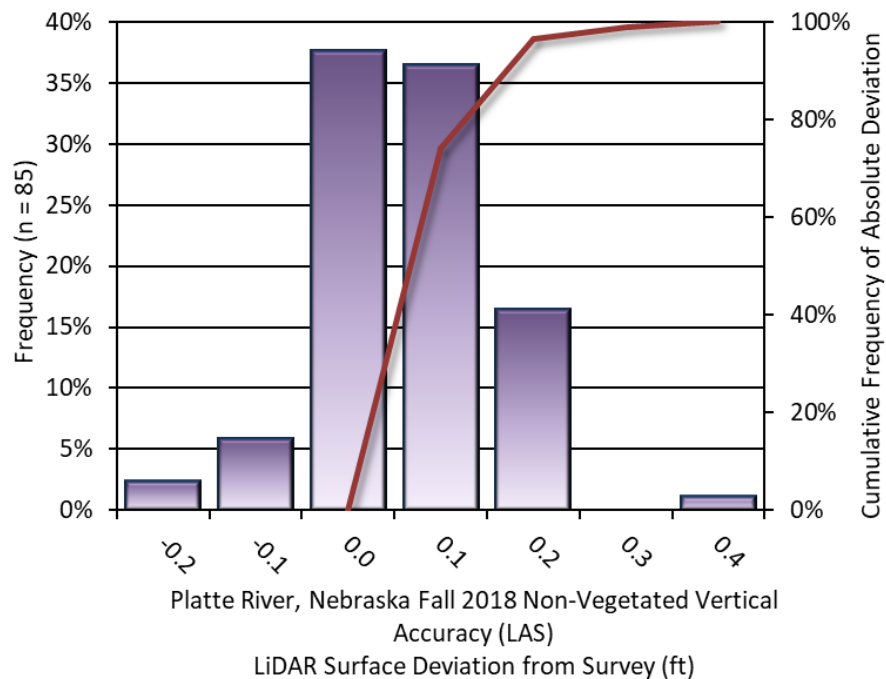


Figure 12: Frequency histogram for LiDAR unclassified las deviation from ground check point values

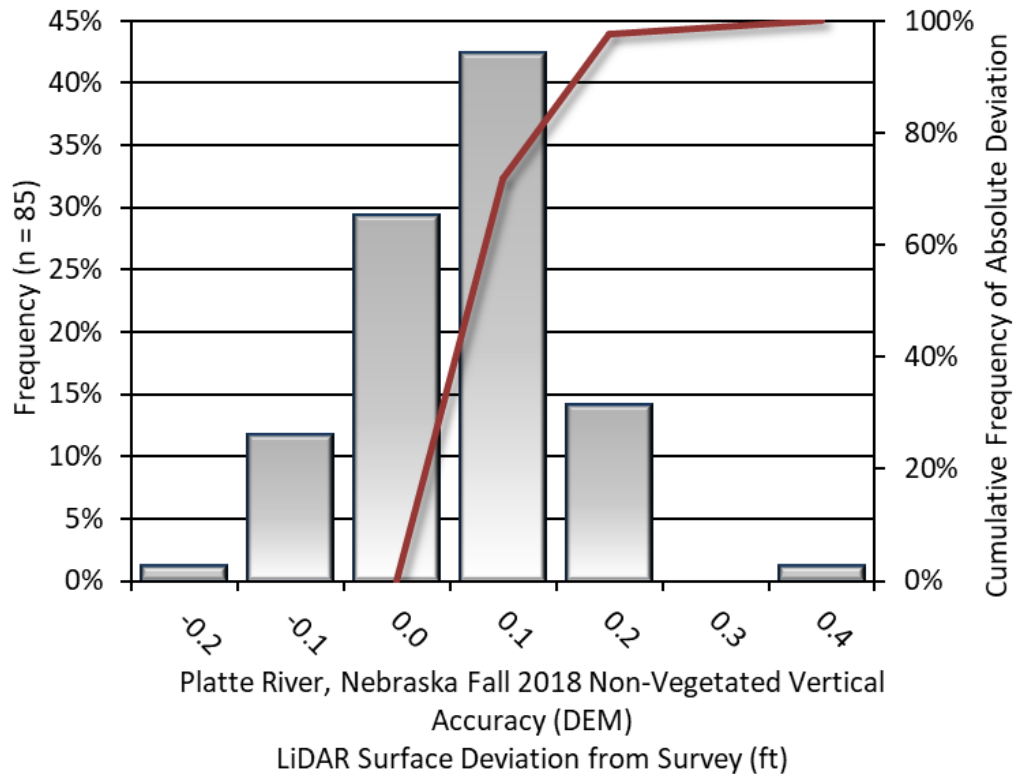


Figure 13: Frequency histogram for LiDAR Bare Earth DEM deviation from ground check point values

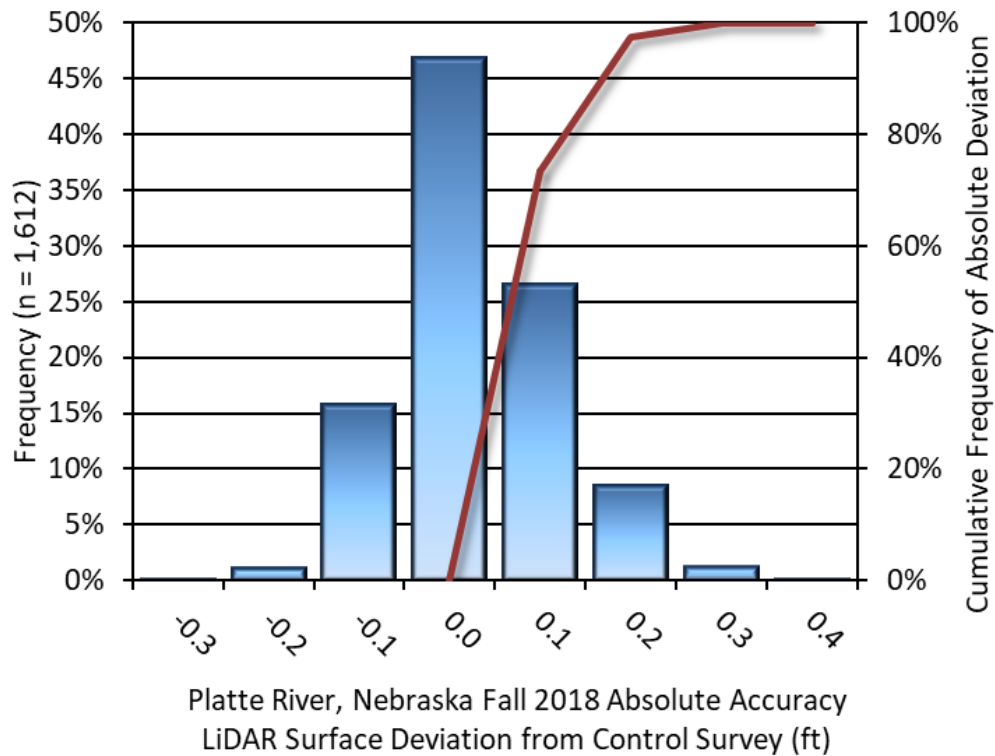


Figure 14: Frequency histogram for LiDAR surface deviation from ground control point values

LiDAR Bathymetric Vertical Accuracies

Submerged bathymetric check points were also collected in order to assess the submerged surface vertical accuracy. Assessment of 58 bathymetric check points resulted in an average vertical accuracy of 0.349 feet (0.107 meters) (Table 11, Figure 15). Below presents bathymetric accuracy results and also includes summary statistics for the submerged bathymetric check points at various depth ranges.

During the collection of the airborne LiDAR data and bathymetric check points QSI surveyors noted a flood event that occurred on October 9, 2018. This event took place after some bathymetric check points were collected but prior to the airborne acquisition of the location and resulted in a shift of over 0.5 meters of sediment where the check points were collected. Because of this event, QSI chose to omit these 10 submerged bathymetric check points from the final bathymetric vertical accuracy assessment. All check points were located between Guendel Island and Grand Island.

Table 11: Bathymetric Vertical Accuracy Results

Submerged Bathymetric Vertical Accuracy for Check Points at Indicated Depth						
	0 - 0.25 ft	0.25 – 0.5 ft	0.5 – 0.75 ft	0.75 – 1.0 ft	> 1.0 ft	Cumulative
Sample	9	9	16	8	16	58
Average DZ	0.001 ft	0.161 ft	0.052 ft	0.068 ft	0.058 ft	0.065 ft
	0.000 m	0.049 m	0.016 m	0.021 m	0.018 m	0.020 m
Median	0.013 ft	0.131 ft	0.043 ft	0.100 ft	0.015 ft	0.043 ft
	0.004 m	0.040 m	0.013 m	0.031 m	0.005 m	0.013 m
RMSE	0.184 ft	0.196 ft	0.132 ft	0.128 ft	0.213 ft	0.176 ft
	0.056 m	0.060 m	0.040 m	0.039 m	0.065 m	0.054 m
Standard Deviation (1σ)	0.195 ft	0.118 ft	0.126 ft	0.116 ft	0.212 ft	0.165 ft
	0.059 m	0.036 m	0.038 m	0.035 m	0.065 m	0.050 m
95th Percentile	0.346 ft	0.324 ft	0.251 ft	0.204 ft	0.430 ft	0.349 ft
	0.105 m	0.099 m	0.077 m	0.062 m	0.131 m	0.107 m

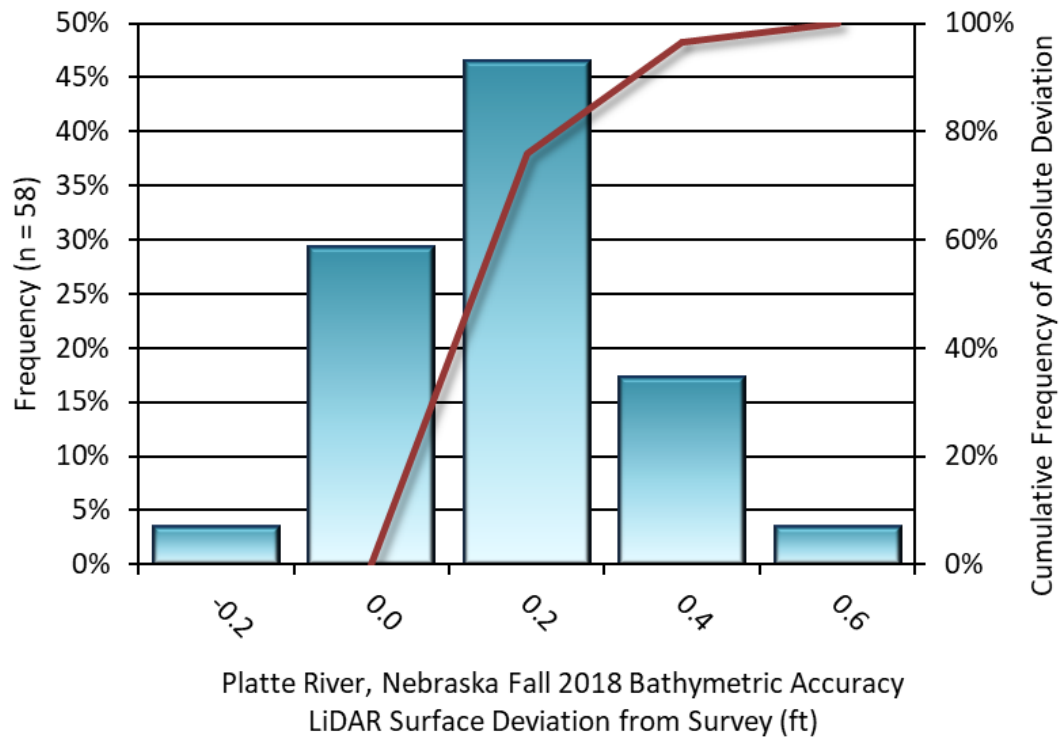


Figure 15: Frequency histogram for LiDAR surface deviation from bathymetric check point values

LiDAR Relative Vertical Accuracy

Relative vertical accuracy refers to the internal consistency of the data set as a whole: the ability to place an object in the same location given multiple flight lines, GPS conditions, and aircraft attitudes. When the LiDAR system is well calibrated, the swath-to-swath vertical divergence is low (<0.10 meters). The relative vertical accuracy was computed by comparing the ground surface model of each individual flight line with its neighbors in overlapping regions. The average (mean) line to line relative vertical accuracy for the Platte River LiDAR project was 0.092 feet (0.028 meters) (Table 12, Figure 16).

Table 12: Relative accuracy results

Relative Accuracy	
Sample	320 surfaces
Average	0.092 ft 0.028 m
Median	0.092 ft 0.028 m
RMSE	0.095 ft 0.029 m
Standard Deviation (1 σ)	0.013 ft 0.004 m
1.96 σ	0.025 ft 0.008 m

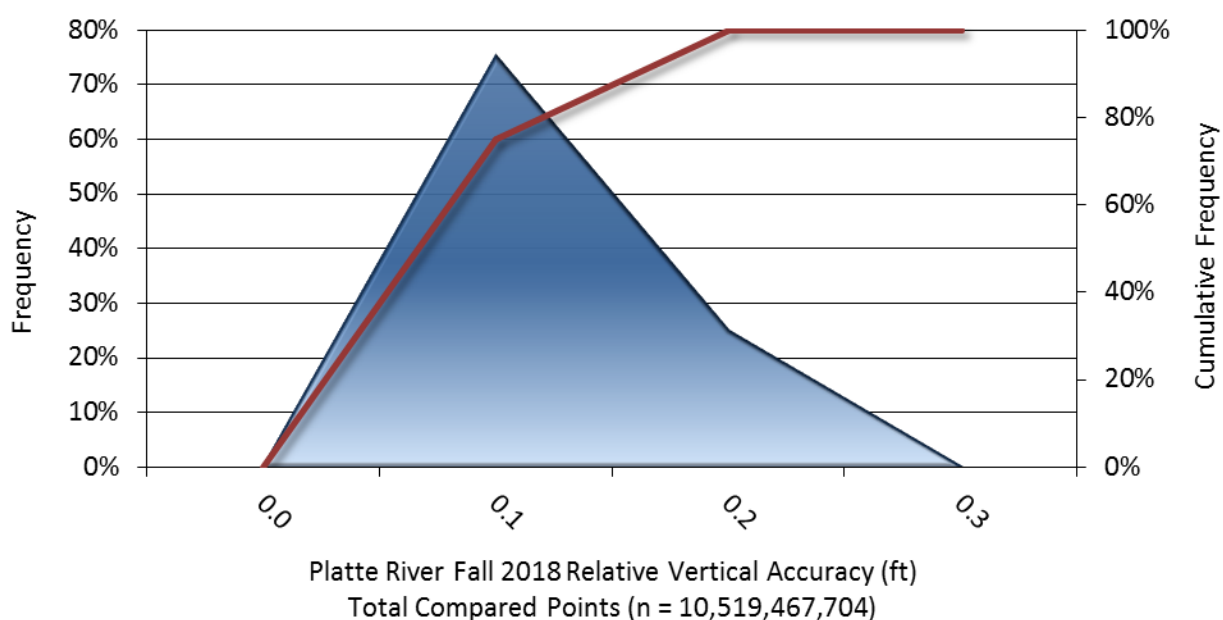


Figure 16: Frequency plot for relative vertical accuracy between flight lines

CERTIFICATIONS

Quantum Spatial, Inc. provided lidar services for the Platte River project as described in this report.

I, Steven Miller, have reviewed the attached report for completeness and hereby state that it is a complete and accurate report of this project.

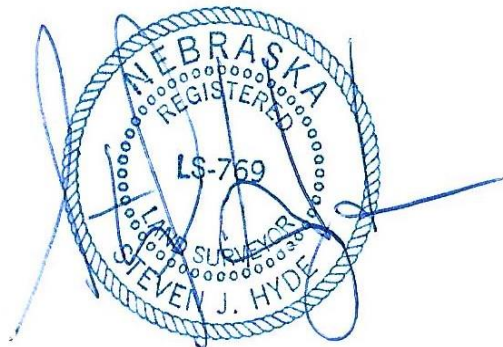
Steven R. Miller
Steven R. Miller (Feb 13, 2019)

Feb 13, 2019

Steven Miller
Project Manager
Quantum Spatial, Inc.

I, Steven J. Hyde, RLS, being duly registered as a Professional Land Surveyor in and by the state of Nebraska, hereby certify that the methodologies, static GNSS occupations used during airborne flights, and ground survey point collection were performed using commonly accepted Standard Practices. QSI field work conducted for this report was conducted between October 3rd and October 10th, 2018.

Accuracy statistics shown in the Accuracy Section of this Report have been reviewed by me and found to meet the "National Standard for Spatial Data Accuracy".



02/07/2019

Steven J. Hyde, RLS# 769
Professional Land Surveyor
Quantum Spatial, Inc.



Figure 17: View looking east over Platte River. The image was created from the LiDAR bare earth model overlaid with the above-ground point cloud and colored by the co-acquired orthoimagery.



Figure 18: View looking west over Platte River. The image was created from the LiDAR bare earth model overlaid with the above-ground point cloud and colored by the co-acquired orthoimagery.

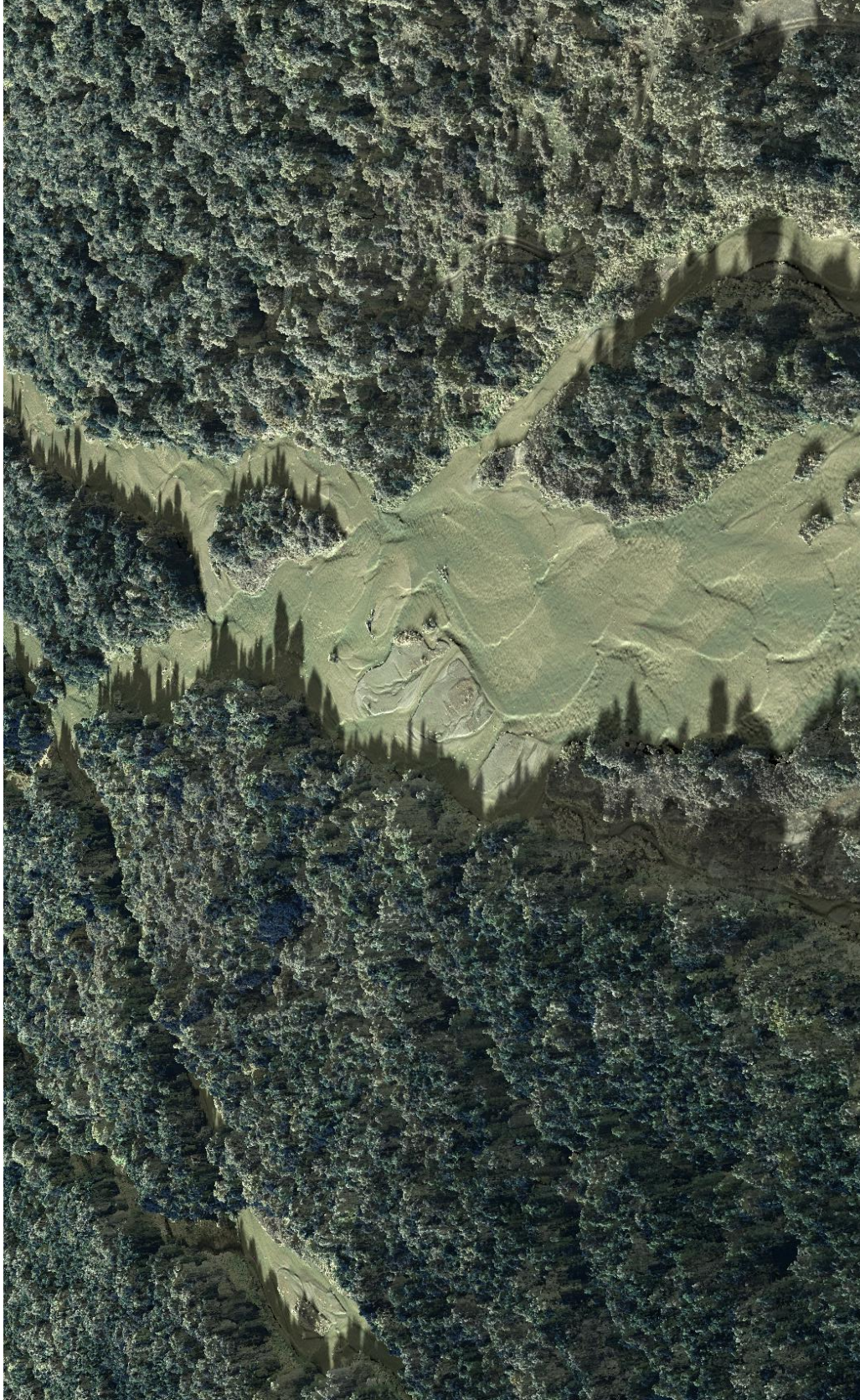


Figure 19: View looking east over Platte River. The image was created from the LiDAR bare earth model overlaid with the above-ground point cloud and colored by the co-acquired orthoimagery.

1-sigma (σ) Absolute Deviation: Value for which the data are within one standard deviation (approximately 68th percentile) of a normally distributed data set.

1.96 * RMSE Absolute Deviation: Value for which the data are within two standard deviations (approximately 95th percentile) of a normally distributed data set, based on the FGDC standards for Non-vegetated Vertical Accuracy (FVA) reporting.

Accuracy: The statistical comparison between known (surveyed) points and laser points. Typically measured as the standard deviation (sigma σ) and root mean square error (RMSE).

Absolute Accuracy: The vertical accuracy of LiDAR data is described as the mean and standard deviation (sigma σ) of divergence of LiDAR point coordinates from ground survey point coordinates. To provide a sense of the model predictive power of the dataset, the root mean square error (RMSE) for vertical accuracy is also provided. These statistics assume the error distributions for x, y and z are normally distributed, and thus we also consider the skew and kurtosis of distributions when evaluating error statistics.

Relative Accuracy: Relative accuracy refers to the internal consistency of the data set; i.e., the ability to place a laser point in the same location over multiple flight lines, GPS conditions and aircraft attitudes. Affected by system attitude offsets, scale and GPS/IMU drift, internal consistency is measured as the divergence between points from different flight lines within an overlapping area. Divergence is most apparent when flight lines are opposing. When the LiDAR system is well calibrated, the line-to-line divergence is low (<10 cm).

Root Mean Square Error (RMSE): A statistic used to approximate the difference between real-world points and the LiDAR points. It is calculated by squaring all the values, then taking the average of the squares and taking the square root of the average.

Data Density: A common measure of LiDAR resolution, measured as points per square meter.

Digital Elevation Model (DEM): File or database made from surveyed points, containing elevation points over a contiguous area. Digital terrain models (DTM) and digital surface models (DSM) are types of DEMs. DTMs consist solely of the bare earth surface (ground points), while DSMs include information about all surfaces, including vegetation and man-made structures.

Intensity Values: The peak power ratio of the laser return to the emitted laser, calculated as a function of surface reflectivity.

Nadir: A single point or locus of points on the surface of the earth directly below a sensor as it progresses along its flight line.

Overlap: The area shared between flight lines, typically measured in percent. 100% overlap is essential to ensure complete coverage and reduce laser shadows.

Pulse Rate (PR): The rate at which laser pulses are emitted from the sensor; typically measured in thousands of pulses per second (kHz).

Pulse Returns: For every laser pulse emitted, the number of wave forms (i.e., echoes) reflected back to the sensor. Portions of the wave form that return first are the highest element in multi-tiered surfaces such as vegetation. Portions of the wave form that return last are the lowest element in multi-tiered surfaces.

Real-Time Kinematic (RTK) Survey: A type of surveying conducted with a GPS base station deployed over a known monument with a radio connection to a GPS rover. Both the base station and rover receive differential GPS data and the baseline correction is solved between the two. This type of ground survey is accurate to 1.5 cm or less.

Post-Processed Kinematic (PPK) Survey: GPS surveying is conducted with a GPS rover collecting concurrently with a GPS base station set up over a known monument. Differential corrections and precisions for the GNSS baselines are computed and applied after the fact during processing. This type of ground survey is accurate to 1.5 cm or less.

Scan Angle: The angle from nadir to the edge of the scan, measured in degrees. Laser point accuracy typically decreases as scan angles increase.

Native LiDAR Density: The number of pulses emitted by the LiDAR system, commonly expressed as pulses per square meter.

APPENDIX A - ACCURACY CONTROLS

Relative Accuracy Calibration Methodology:

Manual System Calibration: Calibration procedures for each mission require solving geometric relationships that relate measured swath-to-swath deviations to misalignments of system attitude parameters. Corrected scale, pitch, roll and heading offsets were calculated and applied to resolve misalignments. The raw divergence between lines was computed after the manual calibration was completed and reported for each survey area.

Automated Attitude Calibration: All data were tested and calibrated using TerraMatch automated sampling routines. Ground points were classified for each individual flight line and used for line-to-line testing. System misalignment offsets (pitch, roll and heading) and scale were solved for each individual mission and applied to respective mission datasets. The data from each mission were then blended when imported together to form the entire area of interest.

Automated Z Calibration: Ground points per line were used to calculate the vertical divergence between lines caused by vertical GPS drift. Automated Z calibration was the final step employed for relative accuracy calibration.

LiDAR accuracy error sources and solutions:

Type of Error	Source	Post Processing Solution
GPS (Static/Kinematic)	Long Base Lines	None
	Poor Satellite Constellation	None
	Poor Antenna Visibility	Reduce Visibility Mask
Relative Accuracy	Poor System Calibration	Recalibrate IMU and sensor offsets/settings
	Inaccurate System	None
Laser Noise	Poor Laser Timing	None
	Poor Laser Reception	None
	Poor Laser Power	None
	Irregular Laser Shape	None

Operational measures taken to improve relative accuracy:

Low Flight Altitude: Terrain following was employed to maintain a constant above ground level (AGL). Laser horizontal errors are a function of flight altitude above ground (about 1/3000th AGL flight altitude).

Focus Laser Power at narrow beam footprint: A laser return must be received by the system above a power threshold to accurately record a measurement. The strength of the laser return (i.e., intensity) is a function of laser emission power, laser footprint, flight altitude and the reflectivity of the target. While surface reflectivity cannot be controlled, laser power can be increased and low flight altitudes can be maintained.

Reduced Scan Angle: Edge-of-scan data can become inaccurate. The scan angle was reduced to a maximum of $\pm 20^\circ$ from nadir, creating a narrow swath width and greatly reducing laser shadows from trees and buildings.

Quality GPS: Flights took place during optimal GPS conditions (e.g., 6 or more satellites and PDOP [Position Dilution of Precision] less than 3.0). Before each flight, the PDOP was determined for the survey day. During all flight times, a dual frequency DGPS base station recording at 1 second epochs was utilized and a maximum baseline length between the aircraft and the control points was less than 13 nm at all times.

Ground Survey: Ground survey point accuracy (<1.5 cm RMSE) occurs during optimal PDOP ranges and targets a minimal baseline distance of 4 miles between GPS rover and base. Robust statistics are, in part, a function of sample size (n) and distribution. Ground survey points are distributed to the extent possible throughout multiple flight lines and across the survey area.

50% Side-Lap (100% Overlap): Overlapping areas are optimized for relative accuracy testing. Laser shadowing is minimized to help increase target acquisition from multiple scan angles. Ideally, with a 50% side-lap, the nadir portion of one flight line coincides with the swath edge portion of overlapping flight lines. A minimum of 50% side-lap with terrain-followed acquisition prevents data gaps.

Opposing Flight Lines: All overlapping flight lines have opposing directions. Pitch, roll and heading errors are amplified by a factor of two relative to the adjacent flight line(s), making misalignments easier to detect and resolve.